Article

Not peer-reviewed version

Topological Properties and Entropy Calculations of Aluminophosphates

Sahaya Vijay J. , Roy S. , Charles Beromeo Bheeter , Mohamad Nazri Husin * , Tony Augustine , Gobithaasan R.U. , Easu Raja M.

Posted Date: 24 April 2023

doi: 10.20944/preprints202304.0845.v1

Keywords: Aluminophosphates; vertex based molecular descriptors; cut method; Shannon's method; correlation coefficient.

Article

Topological Properties and Entropy Calculations of Aluminophosphates

J. Sahaya Vijay [1], S. Roy [1], Charles Beromeo Bheeter [1], Mohamad Nazri Husin [2,*], Tony Augustine [1], R.U. Gobithaasan [2] and M. Easuraja [3]

[1] School of Advanced Sciences, Vellore Institute of Technology, Vellore, India
[2] Special Interest Group on Modelling and Data Analytics (SIGMDA), Faculty of Ocean Engineering Technology and Informatics, Universiti Malaysia Terengganu, Kuala Nerus 21030, Terengganu, Malaysia
[3] Department of Chemistry, Arul Anandar College, Karumathur, India
* Correspondence: nazri.husin@umt.edu.my

Abstract: Topological indices are invariant numerical fields of a graph that give facts about the structure of graphs and are found to be very helpful in predicting the physical properties of aluminophosphates. The characteristics of the aluminophosphates are similar to those of zeolites. Two examples of current applications are natural gas dehydration and humidity sensor. New frameworks are being synthesised by researchers in chemistry and materials science. There are many layers and holes in these substances. In this study, Vertex version of distance-based topological indices, the entropy of topological indices and their numerical analysis are explained.

Keywords: Aluminophosphates; vertex based molecular descriptors; cut method; Shannon's method; correlation coefficient

1. Introduction

Aluminophosphates are essential crystalline microporous materials. Due to its well-defined pore structures and high porosities, it has high permeability, and high selectivity [1,2]. It is available at low prices and provides synthesis and accessibility for various applications. Especially in catalyst preparation, it's used to improve catalyst efficiency and, in process development, to cognize the reaction mechanism [3]. To introduce a particular characteristic in them, aluminophosphates can be incorporated by appropriate metals in the periodic table owing to their outstanding pore attributes, and hydrophilic nature [4]. Accordingly, among solid catalysts, silicoaluminophosphate has a worldwide market of billions of USD per annum [5,6]. Moreover, because of water adsorption properties, potential aluminophosphates are available with a superior pore volume of greater than 14% in contrast to zeolite frameworks. Studying their core structure in a thorough conceptual banner becomes essential to increase the porosity, efficiency, and stability of aluminophosphates for enhanced applications.

Such aluminophosphates materials can be structurally represented using molecular graphs, in which the vertices stand in for atoms and the edges stand in for chemical bonds. To extract topological information from such graphs, one can utilize theoretical graph quantifiers, which in turn give valuable functions that have perfect linear relationships with a variety of properties of such materials through graph invariants or, more commonly, structure descriptors.

Quantitative structure-activity relationships (QSAR) and quantitative structure-property relationships (QSPR) can be supported by topological indices, which are among the structural descriptors that provide numerical functions of a molecules structure. The derived variables can be used to calculate the chemical and biological properties of the materials. The complex systems of such materials that are difficult to define due to their complexity can be viewed as an objective numerical variable that characterises them. The numerical variable that describes the networks of these structural applications is called the topological index of a molecular structure. One of the most significant and efficient structural descriptors in the field of advanced materials is due to the fact that the mathematical functions that can be generated using various graph theoretical approaches can be

Preprints (www.preprints.org) | NOT PEER-REVIEWED | Posted: 24 April 2023 doi:10.20944/preprints202304.0845.v1

used to predict the properties of these materials. They are often an addition to calculations using quantum chemistry that need a deal of computing [18–23]. There is a wide range of indices that can be used in research to understand the relationships between structure and properties .

It should be mentioned that very little progress has been made in the inclusion of topological descriptors that are based purely on the connectivity to chemistry-specific characteristics, such as various indicators [24–38], especially for very heavy atoms in such materials for which relativistic impacts are important.

In his well-known 1948 [39], he first introduced the idea of entropy declaring that the entropy of a probability distribution is known as a measure of the unpredictability. Entropy was used to assess the structural details of graphs and chemical network. Rachhevsky et al. introduced in 1955 the idea of graph entropy on the basis of categorizing vertex orbits [40]. In many disciplines there has been an increase in the use of graph entropy. Information theory was used in biology and chemistry after initial applications in linguistics and electrical engineering. Spontaneous communication is one of the most important innovations [41–45]. A network structural information content was calculated using shannon's entropy formula [39] in light of this realization [46]. This technique has been used to examine living systems using graphs. Graphs are used to investigate biological and chemical networks [47].

In this paper, we study a set of relativistic weighted topological descriptors for chemical molecules. We have also investigated how the perfect linear relationship in $QSPR$ and $QSAR$ models can be improved by assigning optimal weights to the vertices of the structure to obtain a realistic topology. Models that include structural instabilities and other quantum chemistry-derived features that control the overall structural stability of chemical substances have also been explored.

2. Molecular Graph Theoretical Technique

The set of all the edges of G and the set of all the vertices of G are referred to as a graph $G = (V, E)$. There is a cardinality of V and E of G are called as $|V| = M$ and $|E| = N$. The number of edges incident to a is represented by the degree of a vertex a represented as $d_G(a)$. The length of the shortest ab-path is called the distance $d_G(a, b)$ between two vertices $a, b \in V(G)$. We used $d(v)$ and $d(u, v)$ for $d_G(v)$ and $d_G(u, v)$ respectively in this study.

In order to count the vertices and evaluate which quantity is closest to the end vertices of $e = uv$, we must first recall the two numbers based on vertices and edges distance functions.

- $n_u(e) = |t \in V(G) : d(u, t) < d(v, t)|$
- $n_v(e) = |t \in V(G) : d(v, t) < d(u, t)|$

Further we list the distance-based and bond additive topological indices in Table 1 derived from the below mentioned quantitative metrics such as distance and closeness.

Table 1. Different types of vertex-version of distance based molecular descriptors.

Molecular Descriptors	Mathematical Formula
Wiener [17]	$WI_v(G) = \sum_{\{u,v\} \subseteq V(G)} d(u, v)$
Vertex-Szeged [9]	$Sz_v(G) = \sum_{e=uv \in E(G)} n_u(e) n_v(e)$
Vertex-Padmakar-Ivan [12]	$PI_v(G) = \sum_{e=uv \in E(G)} n_u(e) + n_v(e)$
Vertex-Mostar [49]	$Mo_v(G) = \sum_{e=uv \in E(G)} \|n_u(e) - n_v(e)\|$

With matlab programming the provided distance-based and bond additive topological could be successfully calculated based on the Djoković-Winkler relationship on the edge set by finding the equivalence classes of a graph structures. For any two edges $e_1 = ab \in E(G)$ and $e_2 = cd \in E(G)$, if

Preprints (www.preprints.org) | NOT PEER-REVIEWED | Posted: 24 April 2023 doi:10.20944/preprints202304.0845.v1

$d_G(a,c) + d_G(b,d) \neq d_G(a,d) + d_G(b,c)$ then $e_1 \Theta e_2$ is called Djković Winkler relation Θ [48–50] which play a key role in our analytical computation. The graph G that may be isometrically embedded into a hypercube is called a partial cube. Bipartite graphs with transitive Djoković Winkler relation Θ or cut method [51,52] can be used to describe partial cubes [50]. Let Θ^*-class be the transitive closure of Djoković Winkler relation Θ.

The relation Θ is also transitive, hence an equivalence relation if molecular graph G is a partial cube [53]. Let K be a partial cube with its Θ-classes $\mathcal{F}(K) = \{F_1, F_2, ..., F_r\}$. Let $TI \in \{W, W_e, W_{ve}, Sz_v, Sz_e Sz_{ve}, PI, S, Gut, Mo, Mo_e, Mo_t, w^+Mo, w^+Mo_e, w^+Mo_t, w^*Mo, w^*Mo_e.w^*Mo_t\}$, Then $TI(K) = \sum_{i=1}^{k} (TI(K/F_i))$ [53].

In this article, we use the following methods to compute distance based molecular descriptors (See Table 1):

1. $WI_v(G/F_i) = n_1(F_i)n_2(F_i)$
2. $Sz_v(G/F_i) = |F_i|(n_1(F_i)n_2(F_i))$
3. $PI_v(G/F_i) = |F_i|(n_1(F_i) + n_2(F_i))$
4. $Mo_v(G/F_i) = |F_i||(n_1(F_i) - n_2(F_i)|)$

3. Results and Discussion

In this study, we talk about aluminophosphate-based molecular sieve structures and their perfect linear relationships with molecular descriptors. The high selectivity, more significant adsorption velocity, higher strength and increased anti-pollution ability produced by the shape and structural optimization increase the consumption effectiveness of the molecular sieve and widen its service life.

Being the first extra-large-pore crystalline material ever made, the extra-large $VPI-5$, $AIPO$ molecular sieve with 18-ring channels was discovered. The chain-building units used to build $VPI-5$ and $AIPO-H_2$ contain octahedral Al atoms (coordinated with four framework oxygens and two water molecules). The modest number of extra-large-pore microporous materials with 16-ring channels is very noteworthy. The synthesis of $ITQ-51$, a previously unreported extra-large-pore silicoaluminophosphate ($SAPO$) with 16 ring openings, using the bulky aromatic proton sponge $DMAN$ as an $OSDA$ is presented by Martinez-Franco R, et al. [54].

The pore openings of aluminophosphate based molecular sieve structures $T12MR$ (See Figure 1a), $T16MR$ (See Figure 1b) and $VPI-5$ (See Figure 1c) [54] are seems like n mesh. By placing this layer in a n,l,k-dimensional mesh known as a molecular sieve hexagonal mesh $mSHL(n,l,k)$. This layer can be easily stretched to several layers, as shown in Figure 2 and is denoted as G, where G is considered a chemical graph in this study.

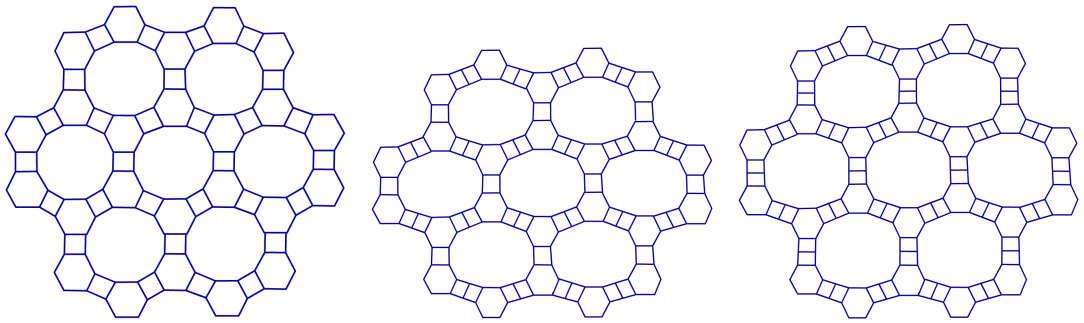

(**a**) $T12MR$ (**b**) $T16MR$ (**c**) $VPI-5$

Figure 1. Aluminophosphate-based molecular sieve structures.

Preprints (www.preprints.org) | NOT PEER-REVIEWED | Posted: 24 April 2023 doi:10.20944/preprints202304.0845.v1

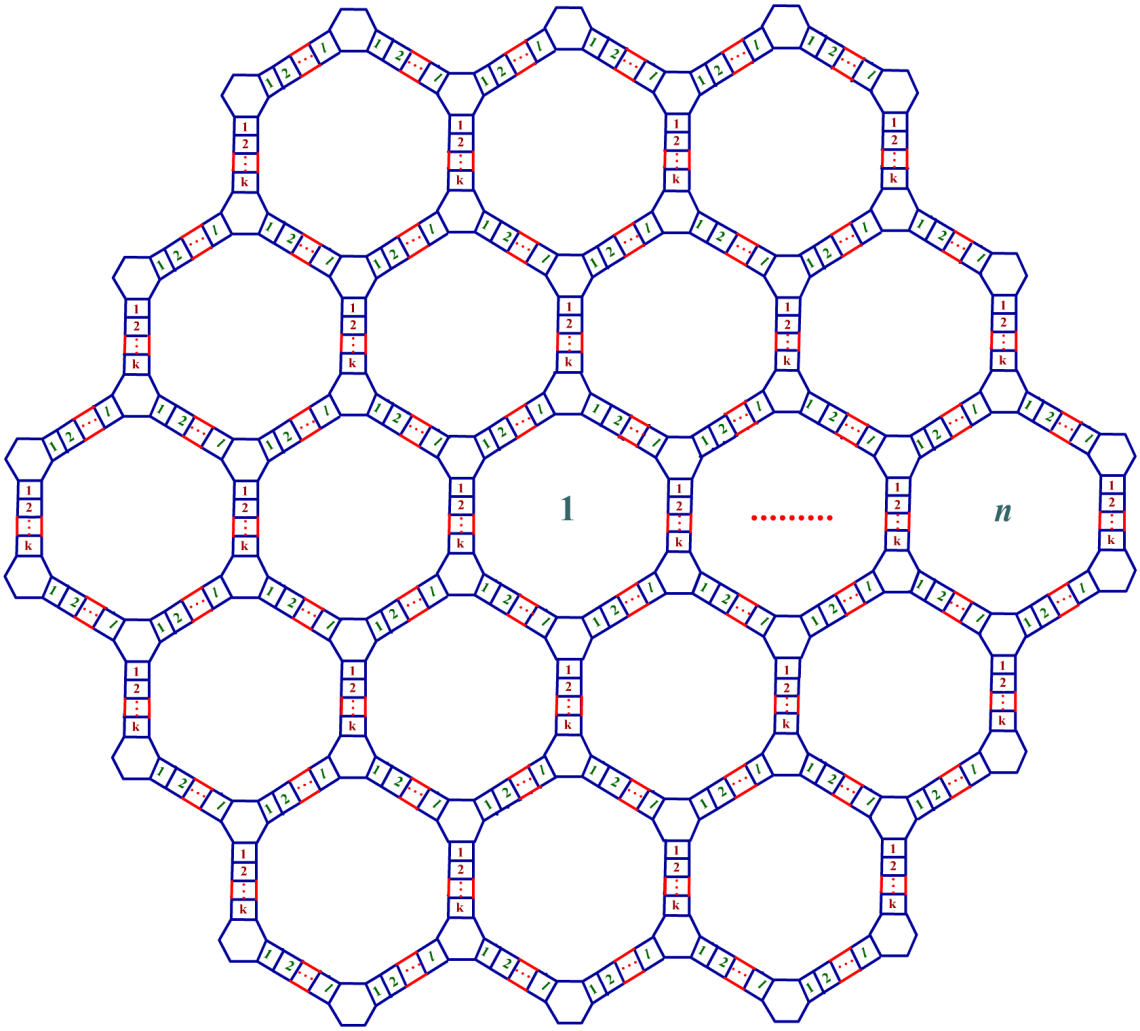

Figure 2. Aluminophosphate-based molecular sieve structure growth $mSHL(n,l,k)$.

Let vertices of G be called atoms, and edges of G are called covalent bonds. Here the total number of vertices of G are denoted as $M = 6n - 2kn - 4ln + 6kn^2 + 12ln^2 + 18n^2$ and the total number of edges of G are denoted as $N = n^2(9k+27) - l(-18n^2+6n) - n(3k-3)$. The graph G that may be isometrically embedded into a hypercube is called a partial cube. Bipartite graphs with transitive Djoković Winkler relation Θ or cut method [51,52] can be used to describe partial cubes [50]. Let Θ^*-class be the transitive closure of Djoković Winkler relation Θ.

Throughout this paper, we discussed two types of Θ^*-classes F_{mi} and F^*_{mi} on G, where $1 \leq m \leq 3$ are depicted in Figure 3. We have shown different directions of Θ^*-classes($Dd(Th)$) on $mSHL(2,1,1)$ in Figure 4. By applying $Dd(Th)$ on G, then G converted to be quotient graphs Q, which is a complete bipartite graph K_2 (See Figure 5). Let $a_jb_j \in K_2$ and $h(i)$ denotes the number of cut edges in G. To accomplish the analytical computation by using all mentioned Θ^*-classes in Figure 4, we now divide the Θ^*-classes of G into two cases.

Case (i): F_{mi} on G; $\{F_{mi}|1 \leq m \leq 3\}$, $\{F_{mi}|1 \leq i \leq n-1\}$, $\{F_{mi}|n \leq i \leq 3n\}$.

For $1 \leq j \leq 4$, $1 \leq i \leq 4$, the vertex-weighted a_j, b_j and the strength-weighted $h(i)$ values on vertices of Q are defined below:

$a_1 = (k+2l+3)i^2 + (2-l-k)i$

$a_2 = i(n(2k+6) + l(4n-1) + 1) - n(k-1) - 2ln^2 - n^2(k+3)$

$a_3 = (k+2l+3)i^2 + (2-2l)i$

$a_4 = i(4ln - k + n(2k+6) + 1) - l(2n^2+2n) + n(k+1) - n^2(k+3)$

$b_j = M - a_j$, where $1 \leq j \leq 4$.

Preprints (www.preprints.org) | NOT PEER-REVIEWED | Posted: 24 April 2023 doi:10.20944/preprints202304.0845.v1

$h(1) = li + 3i$ $\quad h(2) = \frac{((-1)^i+1)}{2}(3n - l + ln + 1) - \frac{((-1)^i-1)}{2}(3n + ln)$

$h(3) = ki + 3i$ $\quad h(4) = \frac{((-1)^i+1)}{2}(3n - k + kn + 1) - \frac{((-1)^i-1)}{2}(3n + kn)$

Case (ii): F^*_{mi} on G; $\{F^*_{mi}|1 \le m \le 3\}$, $\{F^*_{mi}|1 \le j \le n-1, (j-1)l+1 \le i \le jl\}$, $\{F^*_{mi}|nl - l + 1 \le i \le nl\}$, $\{F^*_{mi}|1 \le j \le n-1, (j-1)k+1 \le i \le jk\}$ and $\{F^*_{mi}|nk - k + 1 \le i \le nk\}$

For $5 \le j \le 8, 5 \le i \le 6$, the vertex-weighted a_j, b_j and strength-weighted $h(i)$ values on vertices of Q are defined below:

$a_5 = l(2j^2 - 2j + n(4j-2)) - (2j+2n)(l(j-1) - i + 1) + n(j(2k+6)+2) - j(k-3) + j^2(k+3)$

$a_6 = n^2(3k+9) - l(-6n^2 + 4n) - n(k-5) + n(4i + 4l - 4ln - 4)$

$a_7 = n(j(4l+6)+2) - (2j+2n)(k(j-1) - i + 1) + j^2(2l+3) + k(j^2 - j + n(2j-2)) - j(2l-3)$

$a_8 = n^2(6l+9) - k(-3n^2 + 3n) + n(4i + 4k - 4kn - 4) - n(2l-5)$

$b_j = M - a_j$ where $5 \le j \le 8$

$h(5) = 2n + 2j$ $\quad h(6) = 4n$

By symmetry, we have for $F_{mi^+} = F_{mi^-}$ and $F^*_{mi^+} = F^*_{mi^-}$, for $1 \le m \le 3$. (See Figure 4)

Define,

$$(X(G), \circ) = 2\sum_{i=1}^{n-1} 2h(1)(a_1 \circ b_1) + h(3)(a_3 \circ b_3) + \sum_{i=n}^{3n} 2h(2)(a_2 \circ b_2) + h(4)(a_4 \circ b_4) +$$
$$2[2\sum_{j=1}^{n-1}\sum_{i=(j-1)l+1}^{jl} h(5)(a_5 \circ b_5) + \sum_{i=ln-l+1}^{ln} h(6)(a_6 \circ b_6)] + 2\sum_{j=1}^{n-1}\sum_{i=(j-1)k+1}^{jk} h(5)(a_7 \circ b_7) +$$
$$\sum_{i=kn-k+1}^{kn} h(6)(a_8 \circ b_8),$$ where $(X, \circ) = (W_v, \times), (Sz_v, \times), (PI_v, +)$ and when $(X, \circ) = (W_v, \times)$, $h(i) = 1$, for $1 \le i \le 6$.

$$Y(G) = 2\sum_{i=1}^{n-1} 2h(1)(b_1 - a_1) + h(3)(b_3 - a_3) + \sum_{i=n}^{2n-1} 2h(2)(b_2 - a_2) + h(4)(b_4 - a_4) +$$
$$2[2\sum_{j=1}^{n-1}\sum_{i=(j-1)l+1}^{jl} h(5)(b_5 - a_5) + \sum_{i=\frac{1}{2}(n-l+ln+1)}^{\frac{1}{2}(n)(l+1)} h(6)(b_6 - a_6) + \sum_{i=\frac{1}{2}(ln-l+2)}^{\frac{ln}{2}} h(6)(b_6 - a_6)] +$$
$$2\sum_{j=1}^{n-1}\sum_{i=(j-1)k+1}^{jk} h(5)(b_7 - a_7) + \sum_{i=\frac{1}{2}(n-k+kn+1)}^{\frac{1}{2}(n)(k+1)} h(6)(b_8 - a_8) + \sum_{i=\frac{1}{2}(kn-k+2)}^{\frac{kn}{2}} h(6)(b_8 - a_8).$$

Further, an analytical computation of $(X(G), \circ)$ and $Y(G)$ yields the results of $W_v(G), Sz_v(G), PI_v(G)$ and $Mo_v(G)$.

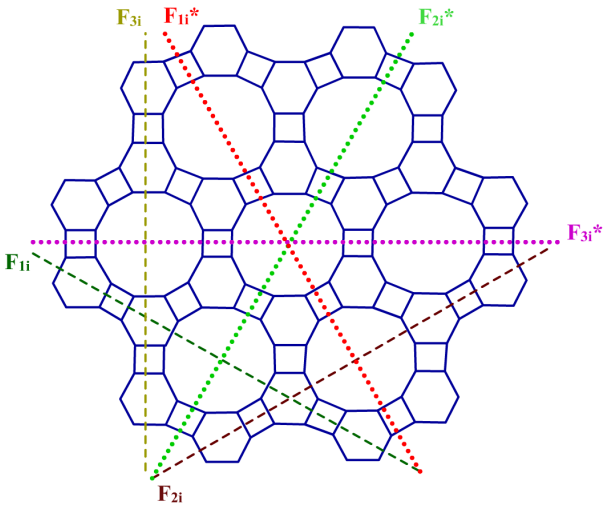

Figure 3. Two types of Θ^*-class F_{fi} and F^*_{fi}.

Preprints (www.preprints.org) | NOT PEER-REVIEWED | Posted: 24 April 2023 doi:10.20944/preprints202304.0845.v1

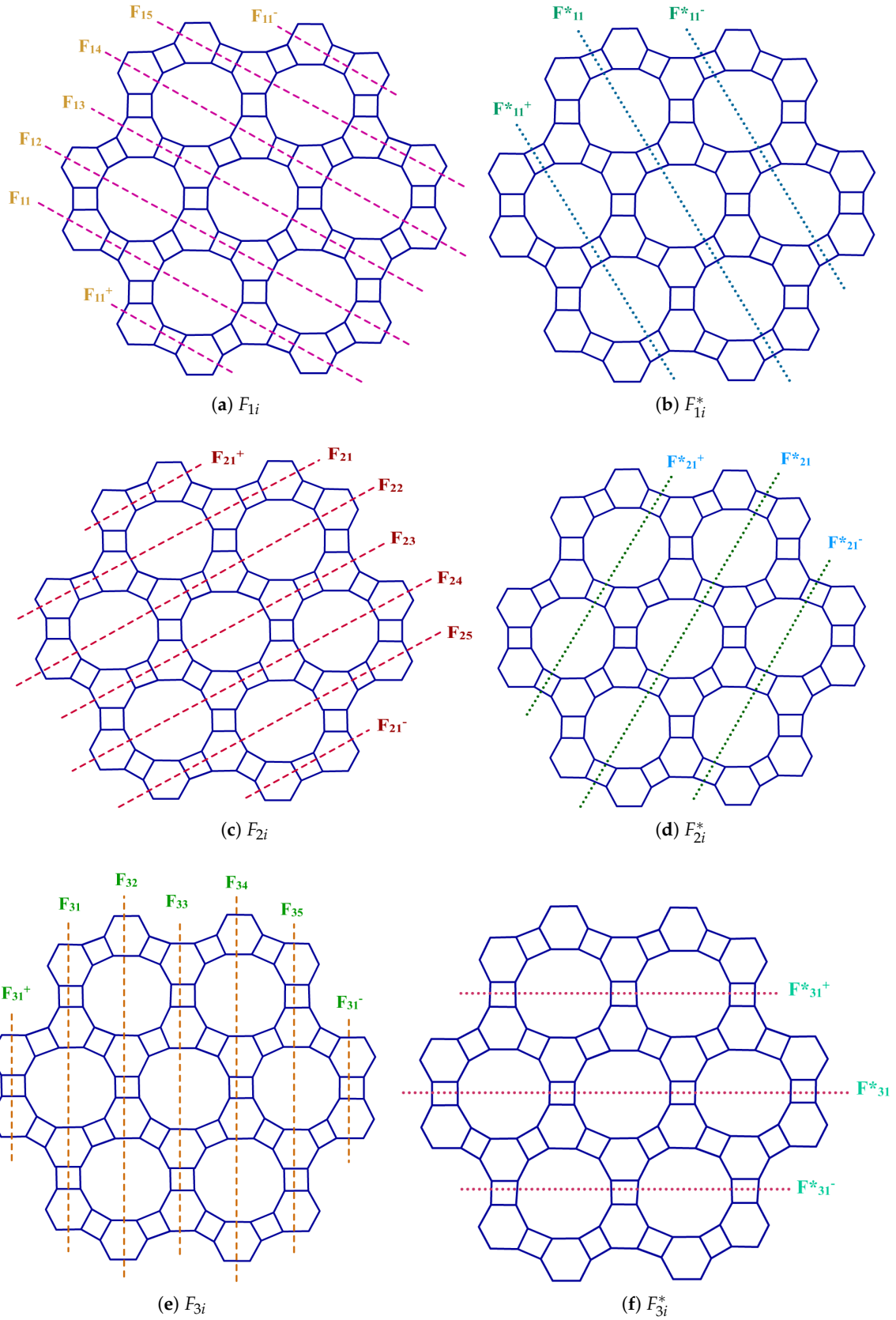

(**a**) F_{1i} (**b**) F^*_{1i}

(**c**) F_{2i} (**d**) F^*_{2i}

(**e**) F_{3i} (**f**) F^*_{3i}

Figure 4. Different directions of Θ^*-classes.

Preprints (www.preprints.org) | NOT PEER-REVIEWED | Posted: 24 April 2023 doi:10.20944/preprints202304.0845.v1

Figure 5. Quotient graph Q.

We obtain, $W_v(G) = \frac{2n}{45}(246k^3n^4 - 270k^3n^3 + 100k^3n^2 - 15k^3n - k^3 + 1476k^2ln^4 - 1230k^2ln^3 + 240k^2ln^2 + 60k^2ln - 6k^2l + 2754k^2n^4 - 1260k^2n^3 - 90k^2n^2 + 90k^2n - 9k^2 + 2952kl^2n^4 - 2265kl^2n^3 + 150kl^2n^2 + 285kl^2n - 42kl^2 + 11016kln^4 - 3870kln^3 - 1620kln^2 + 450kln + 144kl + 9882kn^4 + 1845kn^3 - 1630kn^2 - 345kn + 88k + 1968l^3n^4 - 1770l^3n^3 + 440l^3n^2 + 30l^3n - 8l^3 + 11016l^2n^4 - 4455l^2n^3 - 990l^2n^2 + 405l^2n + 54l^2 + 19764ln^4 + 3690ln^3 - 3260ln^2 - 690ln + 176l + 11502n^4 + 9585n^3 + 1800n^2 - 270n - 72).$

$Sz_v(G) = \frac{n}{60(-1)^k}(174(-1)^kk - 195(-1)^{kn}n - 45(-1)^{3n}(-1)^k + 348(-1)^kl + 2070(-1)^kn - 810(-1)^{kn}n^2 - 1215(-1)^{kn}n^3 + 402(-1)^k - 30(-1)^kk^2 + 10(-1)^kk^3 - 204(-1)^kl^2 - 76(-1)^kl^3 - 45(-1)^k(-1)^n + 9120(-1)^kn^2 + 29700(-1)^kn^3 + 81648(-1)^kn^4 + 87480(-1)^kn^5 - 288(-1)^kkl + 360(-1)^kkn + 100(-1)^kln - 45(-1)^{3n}(-1)^kk^2 + 15(-1)^{3n}(-1)^kk^3 - 90(-1)^{3n}(-1)^kl^2 + 30(-1)^{3n}(-1)^kl^3 + 270(-1)^{3n}(-1)^kn^2 + 2025(-1)^{3n}(-1)^kn^3 + 195(-1)^{kn}(-1)^kn + 810(-1)^{kn}kn^2 - 45(-1)^{kn}k^2n + 405(-1)^(kn)kn^3 - 45(-1)^{kn}k^3n - 60(-1)^{kn}l^2n - 1620(-1)^{kn}ln^3 - 240(-1)^kkl^2 - 96(-1)^kk^2l + 45(-1)^k(-1)^nk - 2760(-1)^kkn^2 + 120(-1)^kk^2n - 5870(-1)^kkn^3 + 120(-1)^kk^3n + 22476(-1)^kkn^4 + 10(-1)^kk^4n + 87480(-1)^kkn^5 + 90(-1)^k(-1)^nl - 7520(-1)^kln^2 + 3240(-1)^kl^2n - 10120(-1)^kln^3 + 120(-1)^kl^3n + 54672(-1)^kln^4 + 174960(-1)^kln^5 - 180(-1)^k(-1)^nn + 810(-1)^{kn}(-1)^kn^2 + 1215(-1)^{kn}(-1)^kn^3 + 90(-1)^{kn}k^2n^2 + 675(-1)^{kn}k^2n^3 - 90(-1)^{kn}k^3n^2 + 135(-1)^{kn}k^3n^3 + 360(-1)^{kn}l^2n^2 - 540(-1)^{kn}l^2n^3 + 45(-1)^{3n}(-1)^kk - 45(-1)^k(-1)^nk^2 - 440(-1)^kk^2n^2 + 15(-1)^k(-1)^nk^3 + 950(-1)^kk^2n^3 - 520(-1)^kk^3n^2 - 8060(-1)^kk^2n^4 - 10(-1)^kk^3n^3 + 160(-1)^kk^4n^2 + 29160(-1)^kk^2n^5 - 540(-1)^kk^3n^4 - 630(-1)^kk^4n^3 + 3240(-1)^kk^3n^5 + 540(-1)^kk^4n^4 + 90(-1)^{3n}(-1)^kl - 90(-1)^k(-1)^nl^2 + 440(-1)^kl^2n^2 + 30(-1)^k(-1)^nl^3 - 8940(-1)^kl^2n^3 + 200(-1)^kl^3n^2 - 36896(-1)^kl^2n^4 + 7380(-1)^kl^3n^3 + 116640(-1)^kl^2n^5 - 24704(-1)^kl^3n^4 + 25920(-1)^kl^3n^5 - 180(-1)^{3n}(-1)^kn + 270(-1)^k(-1)^nn^2 + 2025(-1)^k(-1)^nn^3 + 285(-1)^{kn}kn + 180(-1)^{kn}ln + 80(-1)^kkl^2n^2 - 1480(-1)^kk^2ln^2 - 120(-1)^kk^2l^2n + 11720(-1)^kkl^2n^3 + 4700(-1)^kk^2ln^3 + 960(-1)^kk^3ln^2 - 38000(-1)^kkl^2n^4 - 13904(-1)^kk^2ln^4 - 2520(-1)^kk^3ln^3 + 38880(-1)^kkl^2n^5 + 19440(-1)^kk^2ln^5 + 2160(-1)^kk^3ln^4 - 180(-1)^{3n}(-1)^kkn - 1170(-1)^k(-1)^nkn^2 + 30(-1)^k(-1)^nk^2n + 675(-1)^k(-1)^nkn^3 - 60(-1)^k(-1)^nk^3n - 360(-1)^{3n}(-1)^kln - 2340(-1)^k(-1)^nln^2 + 570(-1)^k(-1)^nl^2n + 1350(-1)^k(-1)^nln^3 - 330(-1)^k(-1)^nl^3n - 240(-1)^{kn}kln - 90(-1)^{kn}(-1)^kk^2n^2 - 675(-1)^{kn}(-1)^kk^2n^3 + 90(-1)^{kn}(-1)^kk^3n^2 - 135(-1)^{kn}(-1)^kk^3n^3 - 360(-1)^{kn}(-1)^kl^2n^2 + 540(-1)^{kn}(-1)^kl^2n^3 + 3680(-1)^kkln + 960(-1)^kk^2l^2n^2 - 2520(-1)^kk^2l^2n^3 + 2160(-1)^kk^2l^2n^4 - 1170(-1)^{3n}(-1)^kkn^2 + 30(-1)^{3n}(-1)^kk^2n + 675(-1)^{3n}(-1)^kkn^3 - 60(-1)^{3n}(-1)^kk^3n - 150(-1)^k(-1)^nk^2n^2 - 225(-1)^k(-1)^nk^2n^3 + 90(-1)^k(-1)^nk^3n^2 - 75(-1)^k(-1)^nk^3n^3 - 2340(-1)^{3n}(-1)^kln^2 + 570(-1)^{3n}(-1)^kl^2n + 1350(-1)^{3n}(-1)^kln^3 - 330(-1)^{3n}(-1)^kl^3n - 240(-1)^k(-1)^nl^2n^2 - 900(-1)^k(-1)^nl^2n^3 + 960(-1)^k(-1)^nl^3n^2 - 600(-1)^k(-1)^nl^3n^3 - 285(-1)^{kn}(-1)^kkn - 180(-1)^{kn}(-1)^kln + 360(-1)^{kn}kln^2 + 60(-1)^{kn}kl^2n + 60(-1)^{kn}k^2ln + 1080(-1)^{kn}kln^3 + 800(-1)^kkln^2 + 520(-1)^kkl^2n + 700(-1)^kk^2ln - 8720(-1)^kkln^3 - 120(-1)^kk^3ln - 41552(-1)^kkln^4 + 116640(-1)^kkln^5 - 180(-1)^k(-1)^nkn - 360(-1)^k(-1)^nln - 150(-1)^{3n}(-1)^kk^2n^2 - 225(-1)^{3n}(-1)^kk^2n^3 + 90(-1)^{3n}(-1)^kk^3n^2 - 75(-1)^{3n}(-1)^kk^3n^3 - 240(-1)^{3n}(-1)^kl^2n^2 - 900(-1)^{3n}(-1)^kl^2n^3 + 960(-1)^{3n}(-1)^kl^3n^2 - 600(-1)^{3n}(-1)^kl^3n^3 - 810(-1)^{kn}(-1)^kkn^2 + 45(-1)^{kn}(-1)^kk^2n - 405(-1)^{kn}(-1)^kkn^3 + 45(-1)^{kn}(-1)^kk^3n + 60(-1)^{kn}(-1)^kl^2n - 360(-1)^{kn}kl^2n^2 + 1620(-1)^{kn}(-1)^kln^3 - 360(-1)^{kn}k^2ln^2 + 540(-1)^{kn}kl^2n^3 + 540(-1)^{kn}k^2ln^3 + 240(-1)^{kn}(-1)^kkln + 1020(-1)^k(-1)^nkln + 1680(-1)^{3n}(-1)^kkl^2n^2 + 780(-1)^{3n}(-1)^kk^2ln^2 - 900(-1)^{3n}(-1)^kkl^2n^3 - 450(-1)^{3n}(-1)^kk^2ln^3 - 360(-1)^{kn}(-1)^kkln^2 - 60(-1)^{kn}(-1)^kkl^2n - 60(-1)^{kn}(-1)^kk^2ln - 1080(-1)^{kn}(-1)^kkln^3 + 1020(-1)^{3n}(-1)^kkln + 120(-1)^k(-1)^nkln^2 -$

Preprints (www.preprints.org) | NOT PEER-REVIEWED | Posted: 24 April 2023 doi:10.20944/preprints202304.0845.v1

$300(-1)^k(-1)^n kl^2n - 210(-1)^k(-1)^n k^2ln - 900(-1)^k(-1)^n kln^3 + 360(-1)^{kn}(-1)^k kl^2n^2 + 360(-1)^{kn}(-1)^k k^2ln^2 - 540(-1)^{kn}(-1)^k kl^2n^3 - 540(-1)^{kn}(-1)^k k^2ln^3 + 120(-1)^{3n}(-1)^k kln^2 - 300(-1)^{3n}(-1)^k kl^2n - 210(-1)^{3n}(-1)^k k^2ln - 900(-1)^{3n}(-1)^k kln^3 + 1680(-1)^k(-1)^n kl^2n^2 + 780(-1)^k(-1)^n k^2ln^2 - 900(-1)^k(-1)^n kl^2n^3 - 450(-1)^k(-1)^n k^2ln^3)$

$PI_v(G) = \frac{n}{2(-1)^k}(9n - 2l - k + 3kn + 6ln + 3)(3(-1)^{3n}(-1)^k + (-1)^{kn}k - 4(-1)^k l + 12(-1)^k n - (-1)^{kn} + (-1)^{kn}(-1)^k + 6(-1)^k - 2(-1)^k k^2 + 3(-1)^k(-1)^n + 108(-1)^k n^2 - 16(-1)^k kn - 24(-1)^k ln - (-1)^{kn}(-1)^k k - (-1)^k(-1)^n k + 36(-1)^k kn^2 + 4(-1)^k k^2 n - 2(-1)^k(-1)^n l + 72(-1)^k ln^2 - (-1)^{3n}(-1)^k k - 2(-1)^{3n}(-1)^k l)$

$Mo_v(G) = \frac{1}{2}(2k^2n - 4kn - 8ln - k^2 - 2l^2 - 2(-1)^n k - 80kn^2 - 72kn^3 + 324kn^4 - 4(-1)^n l - 160ln^2 + 12l^2n - 144ln^3 + 648ln^4 + 24(-1)^n n + 3(-1)^n + 12n^2 + 84n^3 + 486n^4 + 2k + (-1)^n k^2 - 32k^2n^2 - 4k^2n^3 + 54k^2n^4 + 4l - 8(-1)^l n^2 + 2(-1)^n l^2 + 16(-1)^l n^3 - 84l^2n^2 - 88l^2n^3 + 216l^2n^4 - 36n + 36(-1)^n n^2 - 40kln^2 - 160kln^3 + 216kln^4 - 4(-1)^n kn - 8(-1)^n ln - 4(-1)^n l^2 n + 16kln - 16(-1)^l k^2n^2 + 32(-1)^l k^2n^3 + 2k^2n - 4(-1)^n k^2n^2 + 8l^2n - 16(-1)^n l^2n^2 - 8(-1)^n kln + 8kln - 16(-1)^n kln^2) - 3)$

Further, we implement degree-based molecular descriptors of G. Let G be broken into three different edge sets using the methodology of edge set partition(ESP) of molecular descriptors. For understanding, the esp of $mSHL(2,1,1)$ are shown in Figure 6.

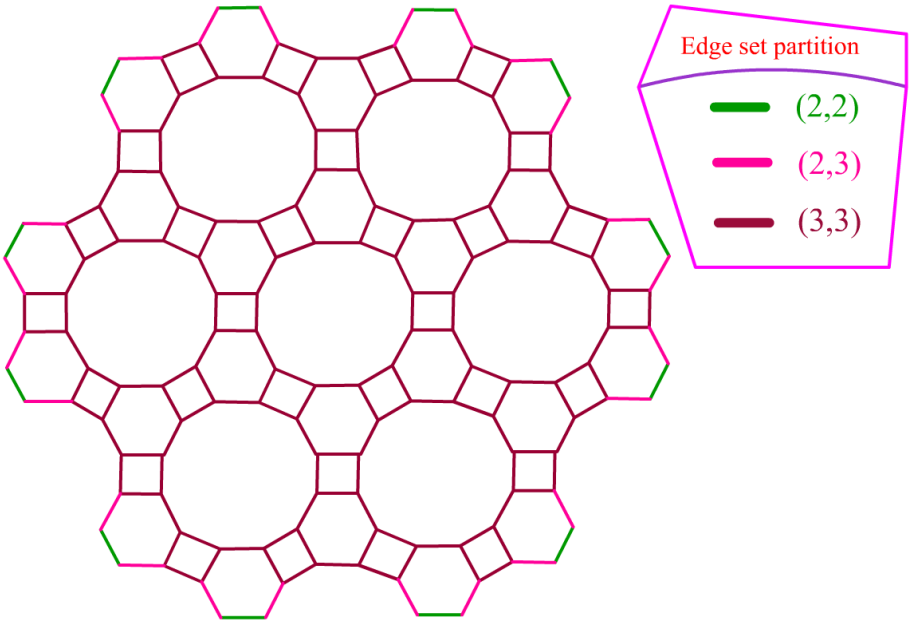

Figure 6. Edge set partitions(ESP).

The esp of G are $|esp(2,2)| = 6n, |esp(2,3)| = 12n, |esp(3,3)| = ((18n^2 - 6n)l + (9k + 27)n^2 - (3k + 15)n)$.

The degree based molecular descriptors [55–63] obtained in Table 2 will help chemists to find the closure values of physiochemical properties by using statistical correlation.

We obtain the results of degree based molecular descriptors from Table 2 by using the above edge set partitions. i.e.,

$M_1(G) = 6n(27n - 6l - 3k + 9kn + 18ln \check{}1)$

$M_2(G) = 3n(81n - 18l - 9k + 27kn + 54ln \check{}13)$

$RM_2(G) = 6n(18n - 4l - 2k + 6kn + 12ln \check{}5)$

$HM(G) = 36n(27n - 6l - 3k + 9kn + 18ln \check{}4)$

$AZ(G) = \frac{9n}{64}(2187n - 486l - 243k + 729kn + 1458ln - 191)$

$R(G) = n(9n - 2l - k + 3kn + 6ln + 26^{\frac{1}{2}} - 2)$

Preprints (www.preprints.org) | NOT PEER-REVIEWED | Posted: 24 April 2023 doi:10.20944/preprints202304.0845.v1

$RR(G) = 3n(27n - 6l - 3k + 9kn + 18ln + 46^{\frac{1}{2}} - 11)$
$RRR(G) = 6n - 2l(-18n^2 + 6n) + 12(2^{\frac{1}{2}})n + 2n^2(9k + 27) - 2n(3k + 15)$
$H(G) = \frac{n}{3}(18n - 4l - 2k + 6kn + 12ln + 11)$
$SC(G) = n(9n - 2l - k + 3kn + 6ln + 26^{\frac{1}{2}} - 2).$

Table 2. Different types of vertex-version of degree based molecular descriptors.

Molecular Descriptors	Mathematical Formula
First Zagreb Index	$M_1(G) = \sum_{uv \in E(G)} [d_u + d_v]$
Second Zagreb Index	$M_2(G) = \sum_{uv \in E(G)} [d_u \times d_v]$
Reduced Second Zagreb Index	$RM_2(G) = \sum_{uv \in E(G)} [(d_u - 1)(d_v - 1)]$
Hyper Zagreb Index	$HM(G) = \sum_{uv \in E(G)} [d_u + d_v]^2$
Augmented Zagreb Index	$AZ(G) = \sum_{uv \in E(G)} [\frac{d_u \times d_v}{d_u + d_v - 2}]^3$
Randić Index	$R(G) = \sum_{uv \in E(G)} [\frac{1}{\sqrt{d_u d_v}}]$
Reciprocal Randić Index	$RR(G) = \sum_{uv \in E(G)} [\sqrt{d_u d_v}]$
Reduced Reciprocal Randić Index	$RRR(G) = \sum_{uv \in E(G)} [\sqrt{(d_u - 1)(d_v - 1)}]$
Harmonic Index	$H(G) = \sum_{uv \in E(G)} [\frac{2}{d_u + d_v}]$
Sum Connectivity Index	$SC(G) = \sum_{uv \in E(G)} \frac{1}{\sqrt{d_u + d_v}}$

By continuing quantitative structural analysis, we have done numerical analysis and the entropy stability of the given molecular descriptors in Table 2. Further provides instructions on calculating entropy values according to Shannon's method by constructing a probability function from degree-based topological indices. We have used Shannon's model to calculate probabilistic entropy because it is the most widely used method 63–67. Using that topological index, the entropy K is calculated as follows:

$$E_k(G) = log(K(G)) - \frac{1}{K(G)} \left(\sum_{uv \in E(G)} (f(e) log(f(e))) \right)$$

By using the $M_1(G)$ to calculate the entropy value for G, the calculation procedure is illustrated.

First Zagreb entropy for molecular graph

$$EM_1(G) = \log(6n(27n - 6l - 3k + 9kn + 18ln - 1)) - \frac{(6n)(2+2)\log(2+2) + (12n)(2+3)\log(2+3)}{6n(27n - 6l - 3k + 9kn + 18ln - 1)}$$
$$+ \frac{((18n^2 - 6n)l + (9k + 27)n^2 - (3k + 15)n)(3+3)\log(3+3)}{6n(27n - 6l - 3k + 9kn + 18ln - 1)}$$
$$= \log(6n(9kn + 18ln - 3k - 6l + 27n - 1)) - \frac{48n\log(2) + 60n\log(5)}{6n(9kn + 18ln - 3k - 6l + 27n - 1)}$$
$$+ \frac{6((18n^2 - 6n)l + (9k + 27)n^2 - (3k + 15)n)\log(6)}{6n(9kn + 18ln - 3k - 6l + 27n - 1)}$$

After simplifying this, we obtain

Preprints (www.preprints.org) | NOT PEER-REVIEWED | Posted: 24 April 2023 doi:10.20944/preprints202304.0845.v1

$$EM_1(G) = \frac{((9k+18l+27)n-3k-6l-1)\log(9((k+2l+3)n-\frac{k}{3}-\frac{2l}{3}-\frac{1}{9})n)}{(9k+18l+27)n-3k-6l-1} + \frac{6\log(2)+14\log(3)-10\log(5)}{(9k+18l+27)n-3k-6l-1}.$$

Each chemical graph's general entropy formulation is too lengthy. Concerning each topological index, the method, and $3D$ plot of entropy (See Figure 7) as mentioned above, makes it easy to generate any degree-based entropies expression.

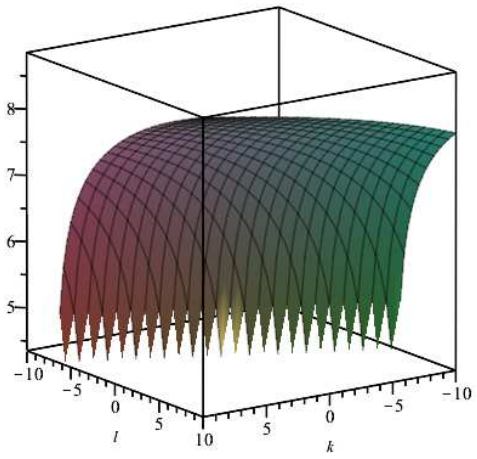

Figure 7. 3D plot of EM_1.

The numerical values of distance and degree-based molecular descriptors utilizing entropy measures generated for G are given in the Tables 3 and 4 with the values of the variable n, l and k ranging from 1 to 10. These values were plotted using the Origin 2020b software for a graphical comparison (See Figures 8–10) of the computed topological descriptors below. The three-dimensional plots can also compare the degree-based indices' behaviour for G.

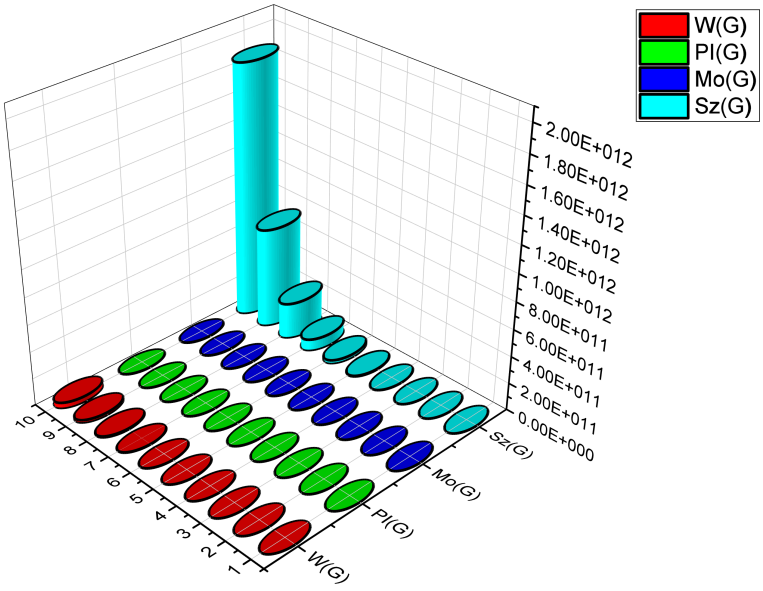

Figure 8. Comparison of graphical representation of distance based molecular descriptors.

Preprints (www.preprints.org) | NOT PEER-REVIEWED | Posted: 24 April 2023 doi:10.20944/preprints202304.0845.v1

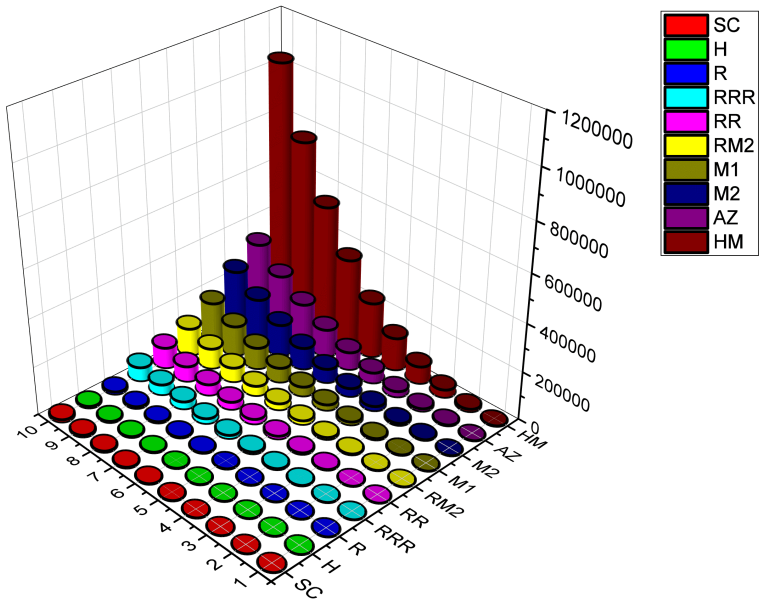

Figure 9. Comparison of graphical representation of degree based molecular descriptors.

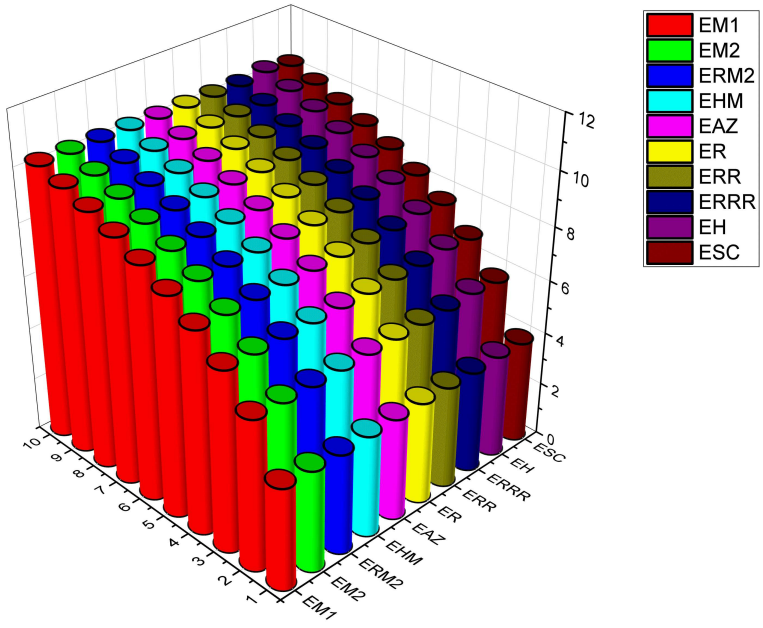

Figure 10. Comparison of entropy measures for G.

Table 3. Numerical values for diistance-based molecular descriptors.

(n, l , k)	**(1, 1, 1)**	**(2, 2, 2)**	**(3, 3, 3)**	**(4, 4, 4)**	**(5, 5, 5)**
$WI_v(G)$	3024	270,000	4,668,072	37,920,768	198,934,944
$Sz_v(G)$	12,096	2,180,550	59,575,584	665,112,240	4,487,610,096
$PI_v(G)$	1728	59,976	560,592	2,819,448	10,144,560
$Mo_v(G)$	576	27,684	265,776	1,385,064	4,916,352
(n, l , k)	**(6, 6, 6)**	**(7, 7, 7)**	**(8, 8, 8)**	**(9, 9, 9)**	**(10, 10, 10)**
$WI_v(G)$	784,272,816	2,527,739,928	7,013,962,368	17,335,729,008	39,076,777,008
$Sz_v(G)$	21,585,912,126	82,522,470,576	2.6439E+11	7.43054E+11	1.87393E+12
$PI_v(G)$	28,958,688	71,033,760	154,482,768	308,200,032	571,213,080
$Mo_v(G)$	14,290,380	34,549,680	76,122,576	149,955,648	280,858,740

Preprints (www.preprints.org) | NOT PEER-REVIEWED | Posted: 24 April 2023 doi:10.20944/preprints202304.0845.v1

Table 4. Numerical values for degree-based molecular descriptors.

(n, l , k)	(1, 1, 1)	(2, 2, 2)	(3, 3, 3)	(4, 4, 4)	(5, 5, 5)
$M_1(G)$	264	1716	5328	12,072	22,920
$M_2(G)$	366	2514	7902	17,988	34,230
$RM_2(G)$	150	1092	3474	7944	15,150
$HM(G)$	1476	10,080	31,644	72,000	136,980
$AZ(G)$	485.71875	3226.78125	10,068.46875	22,856.0625	43,434.84375
$R(G)$	17.899	101.798	305.6969	683.5959	1.29E+03
$RR(G)$	131.3939	856.7878	2.66E+03	6.03E+03	1.15E+04
$RRR(G)$	82.9706	561.9411	1.76E+03	4.00E+03	7.61E+03
$H(G)$	13.66666667	71.33333333	209	462.6666667	868.3333333
$SC(G)$	17.899	101.798	305.6969	683.5959	1.29E+03
(n, l , k)	**(6, 6, 6)**	**(7, 7, 7)**	**(8, 8, 8)**	**(9, 9, 9)**	**(10, 10, 10)**
$M_1(G)$	38,844	60,816	89,808	126,792	172,740
$M_2(G)$	58,086	91,014	134,472	189,918	258,810
$RM_2(G)$	25,740	40,362	59,664	84,294	114,900
$HM(G)$	232,416	364,140	537,984	759,780	1,035,360
$AZ(G)$	73,650.09375	115,347.0938	170,371.125	240,567.4688	327781.4063
$R(G)$	2.18E+03	3.40E+03	5.02E+03	7.07E+03	9.63E+03
$RR(G)$	1.94E+04	3.04E+04	4.49E+04	6.34E+04	8.64E+04
$RRR(G)$	1.29E+04	2.02E+04	2.99E+04	4.22E+04	5.75E+04
$H(G)$	1462	2279.666667	3357.333333	4731	6436.666667
$SC(G)$	2.18E+03	3.40E+03	5.02E+03	7.07E+03	9.63E+03

All numerical value results of molecular descriptors are approaches to the entropy properties of G (See Table 5). The correlation (r) gauge chart shows how strongly two quantitative variables are correlated. Pearson's correlation coefficient (r) is defined as follows.

$$r = \frac{\sum(t_i - t^-)(s_i - s^-)}{\sqrt{\sum(t_i - t^-)^2 \sum(s_i - s^-)^2}}$$

where, r = correlation co-efficient
t_i = values of the t-variable in a sample.
t^- = mean the values of the t-variable.
s_i = values of the s-variable in a sample.
s^- = mean the values of the s-variable.

Table 5. Numerical values for degree-based entropies.

(n, l, k)	$(1,1,1)$	$(2,2,2)$	$(3,3,3)$	$(4,4,4)$	$(5,5,5)$	$(6,6,6)$	$(7,7,7)$	$(8,8,8)$	$(9,9,9)$	$(10,10,10)$
$EM_1(G)$	3.8625	5.6801	6.8006	7.6137	8.2525	8.7787	9.2262	9.6155	9.96	10.269
$EM_2(G)$	3.8383	5.6711	6.7961	7.6111	8.2507	8.7775	9.2253	9.6148	9.9594	10.2685
$ERM_2(G)$	3.7907	5.6552	6.7883	7.6064	8.2477	8.7753	9.2237	9.6135	9.9584	10.2677
$EHM(G)$	3.8404	5.6719	6.7965	7.6113	8.2509	8.7776	9.2254	9.6148	9.9595	10.2685
$EAZ(G)$	3.8576	5.678	6.7995	7.6131	8.2521	8.7784	9.226	9.6153	9.9599	10.2689
$ER(G)$	3.8599	5.6782	6.7995	7.6131	8.2521	8.7784	9.226	9.6153	9.9599	10.268
$ERR(G)$	3.862	5.6798	6.8005	7.6137	8.2525	8.7787	9.2262	9.6155	9.96	10.269
$EH(G)$	3.8928	5.7735	6.9177	7.7412	8.3854	8.9147	9.3642	9.7548	10.1002	10.4098
$ESC(G)$	3.8552	5.6756	6.7976	7.6113	8.2504	8.7769	9.2245	9.6138	9.9584	10.2674

We have done r between degree based descriptors(A) and degree entropy values (B) below the Table 6 and the correlation between A and B is denoted as $A \sim B$.

Preprints (www.preprints.org) | NOT PEER-REVIEWED | Posted: 24 April 2023 doi:10.20944/preprints202304.0845.v1

Table 6. Statistical Correlation (r) between degree based descriptors and degree based entrophy values.

(n, l , k)	$M_1 \sim EM_1$	$M2 \sim EM_2$	$RM_2 \sim ERM_2$	$HM \sim EHM$	$AZ \sim EAZ$
r	0.800895321	0.799930694	0.798222338	0.800014703	0.800664403
(n, l , k)	$R \sim ER$	$RR \sim ERR$	$RRR \sim ERRR$	$H \sim EH$	$SC \sim ESC$
r	0.822763752	0.80086312	0.800240768	0.798861487	0.801363561

The result shows that this study's vertex-based indices are perfect linear relationships. As a result, all the indices mentioned in this study are extremely useful in determining the physiochemical properties and applications of $mSHL(n,l,k)$. As a result, the Randić index is the perfect linear relationship index for $mSHL(n,l,k)$. The effect of this paper, based on applications and properties, is beneficial in getting the scientific results of boric acid structure for future study.

4. Conclusions

This study has computed synthetic structural descriptors for aluminophosphate-based molecular sieve structure $mSHL(n,l,k)$ using cut methods for vertex and edge-weighted molecular graphs. Entropy calculations for degree-based descriptors and linear correlation calculations for $mSHL(n,l,k)$ have been made. Future uses of these materials for catalysis and sorption will be enhanced by topological descriptors of $mSHL(n,l,k)$ that can provide property correlations for rapid computations of their physicochemical properties. Topological methods can also get quantitative data for phase transitions and other material alterations caused by chemical interactions, contaminants, and heavy metal ions. The graphical presentation of this work, the linear correlation, and the numerical comparison of the computed results will be helpful to both theoretical chemists and specialists in the field. Further analysis, we hope our results will support the researcher in predicting the NMR pattern for NMR signal processing. And also it supports the investigators to get new ideas in hypothetical and investigational on NMR Spectroscopy.

Author Contributions: J.S.V.: Data collection, Writing of an original draft preparation, Visualization, Software, Methodology and Investigation. S.R.: Conceptualization, Supervision, Investigation, Reviewing and Editing. C.B.B.: Visualization, Investigation, Reviewing and Editing. M.N.H.: Visualization, Investigation. T.A.: Writing of an original draft preparation, Software. R.U.G.: Conceptualization, Investigation. M.E.: Visualization, Investigation. All authors have read and agreed to the published version of the manuscript.

Funding: The authors would like to thanks Universiti Malaysia Terengganu for the support of this research work via research vot number: 55330.

Data Availability Statement: No data associated in the manuscript.

Acknowledgments: We thank University Malaysia Terengganu for providing funding support for this project (UMT/TAPE-RG/2021/55330).

Conflicts of Interest: The authors declare no competing interests.

Ethical approval: Not applicable.

References

1. Wang, Y.; Zou, X.; Sun, L.; Ronga, H.; Zhu, G. A zeolite-like aluminophosphate membrane with molecular-sieving property for water desalination. *Chem. Sci.* **2018**, *9*, 2533–2539.
2. Yang, M.; Fan, D.; Wei, Y.; Tian, P.; Liu, Z. Recent Progress in Methanol-to-Olefins (MTO) Catalysts. *Adv. Mater. Lett.* **2019**, *31*, 1902181.
3. Huang, Z.; Seo, S.; et.al, 3D-3D topotactic transformation in aluminophosphate molecular sieves and its implication in new zeolite structure generation. *Nat. Commun.* **2020**, *11*, 3762.
4. Yu, J.; Xu, R. Insight into the construction of open-framework aluminophosphates. *Chem. Soc. Rev.* **2006**, *35*, 593–604.
5. Cheetham, A.K.; Férey, G.; Loiseau, T. Open-framework inorganic materials. *Angew. Chem. Int. Ed.* **1999**, *38*, 3268–3292.

6. Liu, Z.; Xu, J.; Xu, M.; et al. Ultralow-temperature-driven water-based sorption refrigeration enabled by low-cost zeolite-like porous aluminophosphate. *Nat. Commun.* **2022**, *13*, 193.
7. Gozalbes, R.; Doucet, P.J.; Derouin, F. Application of topological descriptors in QSAR and drug design: History and new trends. *Curr. Drug Targets Infect. Disord.* **2002**, *2*.
8. Arockiaraj, M.; Clement, J.; Tratnik, N.; Mushtaq, S.; Balasubramanian, K. Weighted Mostar indices as measures of molecular peripheral shapes with applications to graphene, graphyne and graphdiyne nanoribbons. *SAR QSAR Environ. Res.* **2020**, *31*, 187–208.
9. Gutman, I. A Formula for the Wiener Number of Trees and Its Extension to Graphs Containing Cycles. *Graph Theory Notes* **1994**, *27*, 9–15.
10. Gutman, I. Selected properties of the Schultz molecular topological index. *J. Chem. Inf. Comput. Sci.* **1994**, *34*, 1087e1089.
11. Gutman, I.; Ashrafi, A.R. The edge version of the Szeged index. *Croat. Chem. Acta* **2008**, *81*, 263–266.
12. Khadikar, P.V.; Karmarkar, S.; Agrawal, V.K. A novel PI index and its applications to QSPR/QSAR studies. *J. Chem. Inf. Comput. Sci.* **2001**, *41*, 934–949.
13. Khalifeh, M.H.; Yousefi-Azari, H.; Ashrafi, A.R.; Gutman, I. The edge Szeged index of product graphs. *Croat. Chem. Acta* **2008**, *81*, 277–281.
14. Khalifeh, M.H.; Yousefi-Azari, H.; Ashrafi, A.R.; Wagner, S.G. Some new results on distance-based graph invariants. *Eur. J. Combinator.* **2009**, *30*, 1149–1163.
15. Klein, D.J.; Lukovits, I.; Gutman, I. On the definition of the hyper-Wiener index for cycle-containing structures. *J. Chem. Inf. Comput. Sci.* **1995**, *35*, 50–52.
16. Schultz, H.P. Topological organic chemistry. 1. Graph theory and topological indices of alkanes. *J. Chem. Inf. Comput. Sci.* **1989**, *29*, 227–228.
17. Wiener, H. Structural determination of paraffin boiling points. *J. Am. Chem. Soc.* **1947**, *69*, 20.
18. Husin, M.N.; Ariffin, A. On the edge version of topological indices for certain networks. *Ital. J. Pure Appl. Math.* **2022**, *47*.
19. Liu, Y.; Rezaei, M.; Farahani, M.R.; Husin, M.N.; Imran, M. The omega polynomial and the cluj-ilmenau index of an infinite class of the titania nanotubes $TiO_2(m,n)$. *J. Comput. Theor. Nanosci.* **2017**, *14*, 3429–3432.
20. Husin, M.N.; Zafar, S.; Gobithaasan, R.U. Investigation of atom-bond connectivity indices of line graphs using subdivision approach. *Math. Probl. Eng.* **2022**, 6219155.
21. Modabish, A.; Husin, M.N.; Alameri, A.Q.; Ahmed, H.; Alaeiyan, M.; Farahani, M.R.; Cancan, M. Enumeration of spanning trees in a chain of diphenylene graphs. *J. Discrete Math. Sci. Cryptogr.* **2022**, *25*, 241–251.
22. Asif, F.; et al. On Sombor indices of line graph of silicate carbide Si_2 C_3-I[p,q]. *J. Discrete Math. Sci. Cryptogr.* **2022**, *25*, 301–310.
23. Ghani, M.U.; et al. Valency-Based Indices for Some Succinct Drugs by Using M-Polynomial. *Symmetry* **2023**, *15*, 603.
24. Hayat, S.; Wang, S.; Liu, J.B. Valency-based topological descriptors of chemical networks and their applications. *Appl. Math. Model.* **2018**, *60*, 164e178.
25. Gutman, I.; Trinajstic, N. Graph theory and molecular orbitals. Total peelectron energy of alternant hydrocarbons. *Chem. Phys. Lett.* **1972**, *17*, 535–538.
26. Estrada, E.; Torres, L.; Rodríguez, L.; Gutman, I. An atom-bond connectivity index: Modelling the enthalpy of formation of alkanes Indian. *J. Chem.* **1998**, *37*, 849e855.
27. Randić, M. On characterization of molecular branching. *J. Am. Chem. Soc.* **1975**, *97*, 6609e6615.
28. Fajtlowicz, S. On conjectures of graffiti-II congr. *Numer* **1987**, *60*, 187–197.
29. Zhou, B.; Trinajstic, N. On a novel connectivity index. *J. Math. Chem.* **2009**, *46*, 1252–1270.
30. Vukicevic, D.; Furtula, B. Topological index based on the ratios of geometrical and arithmetical means of end-vertex degrees of edges. *J. Math. Chem.* **2009**, *46*, 1369–1376.
31. Albertson, M.O. The irregularity of a graph. *Ars. Comb.* **1997**, *46*, 219e225.
32. Gutman, I.; Togan, M.; Yurttas, A.; Cevik, A.S.; Cangul, I.N. Inverse problem for sigma index. *MATCH Commun. Math. Comput. Chem.* **2018**, *79*, 491–508.
33. Furtula, B.; Gutman, I. A forgotten topological index. *J. Math. Chem.* **2015**, *53*, 1184–1190.
34. Vasilyev, A. Upper and lower bounds of symmetric division deg index. *Iranian J. Math. Chem.* **2014**, *5*, 91–98.

35. Hayat, S.; Imran, M.; Liu, J.-B. An efficient computational technique for degree and distance based topological descriptors with applications. *IEEE Access* **2019**, *7*, 32276–32296.
36. Hayat, S.; Maitla, S.M.; Umair, H.; Wang, S. Distance property of chemical graphs. *Hacet. J. Math. Stat.* **2018**, *47*, 1071–1093.
37. Hayat, S. Computing distance-based topological descriptors of complex chemical networks: New theoretical techniques. *Chem. Phys. Lett.* **2017**, *688*, 51–58.
38. Shirdel, G.H.; Rezapour, H.; Sayadi, A.M. The hyper-Zagreb index of graph operations. *Iranian J. Math. Chem.* **2013**, *4*, 213–220.
39. Shannon, C.E., A mathematical theory of communication. *Bell Syst. Tech. J.* **1948**, *27*, 379–423.
40. Rashevsky, N. Life, information theory, and topology. *Bull. Math. Biol.* **1955**, *17*, 229–235.
41. Dehmer, M.; Graber, M. The discrimination power of molecular identification numbers revisited. *MATCH Commun. Math. Comput. Chem.* **2013**, *69*, 785–794.
42. Ulanowicz, R.E. Quantitative methods for ecological network analysis. *Comput. Biol. Chem.* **2004**, *28*, 321–339.
43. Morowitz, H. Some order-disorder considerations in living systems. *Bull. Math. Biophys.* **1953**, *17*, 81–86.
44. Quastler, H. Information theory in biology. *Bull. Math. Biol.* **1954**, 183–185.
45. Bonchev, D. *Complexity in Chemistry, Introduction and Fundamentals*; Taylor and Francis: Boca Raton, FL, USA, 2003.
46. Sol, R.V.; Valverde, S.I. Information theory of complex networks: On evolution and architectural constraints. *Complex Netw. Lect. Notes Phys.* **2004**, *650*, 189–207.
47. Manzoor, S.; Siddiqui, M.K.; Ahmad, S. On entropy measures of molecular graphs using topological indices. *Arab. J. Chem.* **2020**, *13*, 6285–6298.
48. Djoković, D. Distance preserving subgraphs of hypercubes. *J. Combin. Theory Ser. B* **1973**, *14*, 263–267.
49. Došlić, T.; Martinjak, I.; Škrekovski, R.; Spužević, S.T.; Zubac, I. Mostar index. *J. Math. Chem.* **2018**, *56*, 2995–3013.
50. Winkler, P. Isometric embeddings in products of complete graphs. *Discr. Appl. Math.* **1984**, *7*, 221–225.
51. Klavzar, S.; Gutman, I.; Mohar, B. Labeling of benzenoid systems which reflects the vertex-distance relations. *J. Chem. Inf. Comput. Sci.* **1995**, *35*, 590–593.
52. Nadjafi-Arani, M.J.; Klavzar, S. Cut method and Djoković-Winkler's relation. *Electron. Notes Discrete Math.* **2014**, *45*, 153–157.
53. Arockiaraj, M.; Clement, J.; Paul, D.; Balasubramanian, K. Relativistic distance-based topological descriptors of Linde type A zeolites and their doped structures with very heavy elements. *Mol. Phys.* **2020**, e1798529.
54. Martínez-Francoa, R.; et al. Synthesis of an extra-large molecular sieve using proton sponges as organic structure-directing agents Raquel. *Proc. Natl. Acad. Sci. USA* 2012.
55. Balasubramanian, K. Combinatorics, big Data, neural network and AI for medicinal chemistry and drug administration. *Lett. Drug Des. Discov.* **2021**, *18*, 943–948.
56. Sabirov, D.S.; Shepelevich, I.S. Information entropy in chemistry: An overview. *Entropy* **2021**, *23*, e23101240.
57. Chaudhry, F.; Shoukat, I.; Afzal, D.; Park, C.; Cancan, M.; Farahani, M.R. M-Polynomials and degree-Based topological indices of the molecule copper(I) oxide. *J. Chem.* **2021**, 6679819.
58. Mowshowitz, A.; Dehmer, M. Entropy and the complexity of graphs revisited. *Entropy* **2012**, *14*, 559–570.
59. Kavitha, S.R.J.; Abraham, J.; Arockiaraj, M.; Jency, J.; Balasubramanian, K. Topological Characterization and graph entropies of tessellations of kekulene structures: Existence of isentropic structures and applications to thermochemistry, nuclear magnetic resonance, and electron spin resonance. *J. Phys. Chem. A* **2021**, *125*, 8140–8158.
60. Arockiaraj, M.; Paul, D.; Klavžar, S.; Clement, J.; Tigga, S.; Balasubramanian, K. Relativistic distance based and bond additive topological descriptors of zeolite RHO materials. *J. Mol. Struct.* **2022**, *1250*, 131798.
61. Gutman, I. Degree-based topological indices. *Croat. Chem. Acta* **2013**, *86*, 351–361.
62. Arockiaraj, M.; Clement, J.; Tratnik, N. Mostar indices of carbon nanostructures and circumscribed donut benzenoid systems. *Int. J. Quantum Chem.* **2019**, *119*, e26043.
63. Augustine, T.; Roy, S. Topological study on triazine-based covalent-organic frameworks. *Symmetry* **2022**, *14*, 1590.
64. Rahul, M.P.; Clement, J.; Junias, J.S.; Arockiaraj, M.; Balasubramanian, K. Degree-based entropies of graphene, graphyne and graphdiyne using Shannon's approach. *J. Mol. Struct.* **2022**, *1260*, 132797.
65. Sabirov, D.S.; Shepelevich, I.S. Information entropy in chemistry: An overview. *Entropy* **2021**, *23*, 1240.

66. Mowshowitz, A.; Dehmer, M. Entropy and the Complexity of Graphs Revisited. *Entropy* **2012**, *14*, 559–570.
67. Hussain, Z.; Ijaz, N.; Tahir, W.; Butt, M.T.; Talib, S. Calculating degree based multiplicative topological indices of alcohol. *SSRN Electron. J.* **2018**.